

# The Crystal Structure of 1-D-*myo*-Inositol 2-Acetamido-2-deoxy- $\alpha$ -D-glucopyranoside Deacetylase (MshB) from *Mycobacterium tuberculosis* Reveals a Zinc Hydrolase with a Lactate Dehydrogenase Fold\*

Received for publication, August 12, 2003, and in revised form, September 3, 2003  
Published, JBC Papers in Press, September 4, 2003, DOI 10.1074/jbc.M308914200

Jason T. Maynes<sup>‡§</sup>, Craig Garen<sup>‡</sup>, Maia M. Cherney<sup>‡</sup>, Gerald Newton<sup>¶</sup>, Dorit Arad<sup>||</sup>,  
Yossef Av-Gay<sup>||\*\*</sup>, Robert C. Fahey<sup>¶</sup>, and Michael N. G. James<sup>‡ ‡‡</sup>

From the <sup>‡</sup>Canadian Institutes of Health Research, Group in Protein Structure and Function, Department of Biochemistry, Faculty of Medicine, University of Alberta, Edmonton, Alberta T6G 2H7, Canada, the <sup>¶</sup>Department of Chemistry and Biochemistry, University of California, San Diego, La Jolla, California 92093, and the <sup>||</sup>Department of Medicine, University of British Columbia, Vancouver, British Columbia V5Z 2J5, Canada

**Mycothioliol (1-D-*myo*-inositol 2-(N-acetyl-L-cysteinylo-amido-2-deoxy- $\alpha$ -D-glucopyranoside, MSH or AcCys-GlcN-insitol (Ins)) is the major reducing agent in actinomycetes, including *Mycobacterium tuberculosis*. The biosynthesis of MSH involves a deacetylase that removes the acetyl group from the precursor GlcNAc-Ins to yield GlcN-Ins. The deacetylase (MshB) corresponds to Rv1170 of *M. tuberculosis* with a molecular mass of 33,400 Da. MshB is a Zn<sup>2+</sup> metalloprotein, and the deacetylase activity is completely dependent on the presence of a divalent metal cation. We have determined the x-ray crystallographic structure of MshB, which reveals a protein that folds in a manner resembling lactate dehydrogenase in the N-terminal domain and a C-terminal domain consisting of two  $\beta$ -sheets and two  $\alpha$ -helices. The zinc binding site is in the N-terminal domain occupying a position equivalent to that of the NAD<sup>+</sup> co-factor of lactate dehydrogenase. The Zn<sup>2+</sup> is 5 coordinate with 3 residues from MshB (His-13, Asp-16, His-147) and two water molecules. One water would be displaced upon binding of substrate (GlcNAc-Ins); the other is proposed as the nucleophilic water assisted by the general base carboxylate of Asp-15. In addition to the Zn<sup>2+</sup> providing electrophilic assistance in the hydrolysis, His-144 imidazole could form a hydrogen bond to the oxyanion of the tetrahedral intermediate. The extensive sequence identity of MshB, the deacetylase, with mycothiol S-conjugate amidase, an amide hydrolase that mediates detoxification of mycothiol S-conjugate xenobiotics, has allowed us to construct a faithful model of the catalytic domain of mycothiol S-conjugate amidase based on the structure of MshB.**

It is estimated that there are currently 2.2 billion people infected with *Mycobacterium tuberculosis* (TB)<sup>1</sup> worldwide, leading to ~2 million deaths annually (1, 2). To compound the urgency of this situation, 2% of TB clinical isolates display resistance to the common anti-TB medications, isoniazid and rifampicin (3). The latter of these two drugs was the one most recently introduced, in 1968. Clearly, the lack of new anti-TB drugs is a significant problem since the frequency of antibiotic-resistant TB is growing. To develop new anti-TB drugs, we have sought novel metabolic pathways or metabolic intermediates used by the bacteria. One such potential target is mycothiol (1-D-*myo*-inositol 2-(N-acetyl-L-cysteinylo-amido-2-deoxy- $\alpha$ -D-glucopyranoside, MSH or AcCys-GlcN-Ins) (Fig. 1), the reducing agent exclusively present in the order actinomycetes, to which TB belongs (4). This thiol is proposed to have a role similar to that of glutathione in controlling the levels of cellular reactive oxygen species, as an enzyme cofactor and as a potential reactant used for antibiotic removal from the bacteria (5–8). Loss of mycothiol in mycobacteria is associated with slow growth and increased sensitivity to both reactive oxygen species and antibiotics (9).

The biosynthetic pathway of mycothiol involves four steps: 1) production of 1-D-*myo*-inositol-2-acetamido-2-deoxy- $\alpha$ -D-glucopyranose (GlcNAc-Ins) using the glycosyltransferase coded for by Rv0486 (MshA) (10), 2) deacetylation of GlcNAc-Ins by MshB to produce 1-D-*myo*-inositol 2-amino-2-deoxy- $\alpha$ -D-glucopyranoside (GlcN-Ins) (11), 3) the addition of cysteine to the free amine of glucosamine in an ATP-dependent manner to produce Cys-GlcN-Ins, by MshC (Rv2130c) (12), and 4) acetylation of the amine of cysteine by acetyl-CoA (AcCys-GlcN-Ins) by MshD (Rv0819) (13).

We have solved the x-ray crystal structure of mycothiol deacetylase (MshB, TB gene Rv1170), an enzyme involved in the biosynthetic pathway of mycothiol. Recently, it was shown that *Mycobacterial* knockouts lacking MshB activity were more susceptible to reactive oxygen species but also more resistant to isoniazid (14). The extensive sequence similarity of MshB to mycothiol S-conjugate amidase (Mca, TB gene Rv1082) has allowed us to build a faithful comparative molecular model of the latter. Mca may assist in the removal of antibiotics from the infectious bacteria by cleaving the S-conjugate formed by the reaction of MSH and an anti-

\* This work was supported by Grant MGP-37770 from the Canadian Institutes of Health Research (to M. N. G. J.) and by equipment funds from the Alberta Heritage Foundation for Medical Research. The costs of publication of this article were defrayed in part by the payment of page charges. This article must therefore be hereby marked "advertisement" in accordance with 18 U.S.C. Section 1734 solely to indicate this fact.

The atomic coordinates and structure factors (code 1Q74) have been deposited in the Protein Data Bank, Research Collaboratory for Structural Bioinformatics, Rutgers University, New Brunswick, NJ (<http://www.rcsb.org/>).

§ A Pfizer M.D./Ph.D Student. Supported by an M.D./Ph.D Training Award from the Canadian Institutes of Health Research and the Canadian Gene Cure Foundation and supplemental funding from the Alberta Heritage Foundation for Medical Research.

\*\* Supported by the British Columbia Lung Association. A British Columbia Lung-Canadian Institutes of Health Research Scholar.

‡‡ Canada Research Chair in Protein Structure and Function. To whom correspondence should be addressed. Tel.: 780-492-4550; Fax: 780-492-0886; E-mail: Michael.James@ualberta.ca.

<sup>1</sup> The abbreviations used are: TB, tuberculosis; MSH, 1-D-*myo*-inositol 2-(N-acetyl-L-cysteinylo-amido-2-deoxy- $\alpha$ -D-glucopyranoside; Mca, mycothiol S-conjugate amidase; Ins, inositol.

biotic, thereby assisting in the export of the latter from the cell (8, 15).

#### EXPERIMENTAL PROCEDURES

**Protein Expression and Purification**—The expression plasmid was used as described previously (11). Protein was expressed overnight at room temperature by inducing with 0.4 mM isopropyl-1-thio- $\beta$ -D-galactopyranoside in *Escherichia coli* BL21(DE3) cells. Protein purification proceeded using the His<sub>6</sub> tag present on the recombinant protein using a nickel-nitrilotriacetic acid affinity column and 150 mM imidazole elution buffer.

**Crystal Growth**—Crystals of MshB were obtained by the vapor-diffusion method with a mother liquor consisting of 15% polyethylene glycol 4000, 50 mM Tris-HCl (pH = 8.0), 0.1 M Mg(NO<sub>3</sub>)<sub>2</sub>, 6% 1,6-hexanediol, and 10% ethylene glycol. A 1:2 ratio of protein solution (6 mg/ml) to mother liquor was mixed and left for vapor equilibration. Triclinic crystals formed after approximately 1 week at room temperature (Table I).

**Data Collection and Heavy Atom Derivatives**—A high resolution native data set was collected at beamline 8.3.1 at the Advanced Light Source in Berkeley, CA equipped with an ADSC Q210 detector. A heavy atom derivative was obtained by soaking crystals in 1 mM uranyl nitrate for 2 days. The derivative data set was collected on a Rigaku RU-H3R rotating anode generator equipped with a Rigaku R-AXIS IV++ image plate detector. The data were processed using MOSFLM (version 6.11) and scaled with SCALA (16–18). Four heavy atom sites in the asymmetric unit were located using SOLVE via the single isomorphous replacement with anomalous scattering method (19). Solvent flattening and phase extension were done using RESOLVE (20). An initial model was built using aRP-wARP, which traced an initial 987 residues (21). The structure was then subjected to iterative rounds of

refinement with a maximum likelihood target using REFMAC (22) and model fitting using XFIT (23).

**Figures**—All figures were produced using Pymol (24).

**Coordinates**—The atomic coordinates and structure factors have been deposited in the Protein Data Bank with accession code 1Q74.

#### RESULTS

**Crystallography of MshB**—The enzyme crystallized in the triclinic space group P<sub>1</sub> with cell dimensions  $a = 56.8 \text{ \AA}$ ,  $b = 74.0 \text{ \AA}$ ,  $c = 85.6 \text{ \AA}$ ,  $\alpha = 102.1^\circ$ ,  $\beta = 108.2^\circ$ ,  $\gamma = 97.2^\circ$ . There were four protein molecules in the unit cell (asymmetric unit), giving a solvent content of 50% ( $V_M = 2.5 \text{ \AA}^3/\text{Da}$ ). The four molecules present were almost identical with a maximal pairwise C <sub>$\alpha$</sub>  root mean square deviation of 0.30  $\text{Å}$  over a minimum of 251 C <sub>$\alpha$</sub>  atoms. All four molecules are missing two surface loops (minimally residues 100–103 and 164–167), which had untraceable electron density (see Fig. 2, *a* and *b*). Both of these regions are not located near the active site. Additionally, three of the four molecules are missing a surface loop minimally from residues 211–216. This loop is located proximal to the active site but is not expected to play a role in substrate binding or catalysis (see below). The one copy of MshB that contains this loop then represents the most complete model present for the protein. All four molecules are identical in the active site region and contain a catalytic zinc atom.

**Overall Structure of MshB**—MshB consists of one large nine-stranded mixed  $\beta$ -sheet and one small three-stranded anti-parallel  $\beta$ -sheet (Fig. 2, *a* and *b*). The first five strands of the large  $\beta$ -sheet with the associated  $\alpha$ -helices ( $\alpha_1$  to  $\alpha_5$ ) adopt a topology that closely resembles the Rossmann fold of lactate dehydrogenase (25). Several lines of evidence confirm that MshB is a zinc-binding protein (see below). Despite the diverse functions of lactate dehydrogenase (an oxidoreductase) and MshB (a zinc hydrolase), these enzymes adopt a similar fold. The three-dimensional structure of MshB does not have a related fold among the Zn<sup>2+</sup>-dependent metalloenzymes (see below) (structural relationships were searched by the DALI server, but no significantly similar metalloproteins were found (26)). The structure shows that there is a metal binding site comprised of residues from the C terminus of  $\beta$ -strand 1 and the loop linking strand 1 to the helix  $\alpha_1$  (His-13 and Asp-16) as well as His-147 from the N terminus of helix  $\alpha_5$ . In addition, in the holoenzyme, there are two water molecules that coordinate to the Zn<sup>2+</sup> ion,

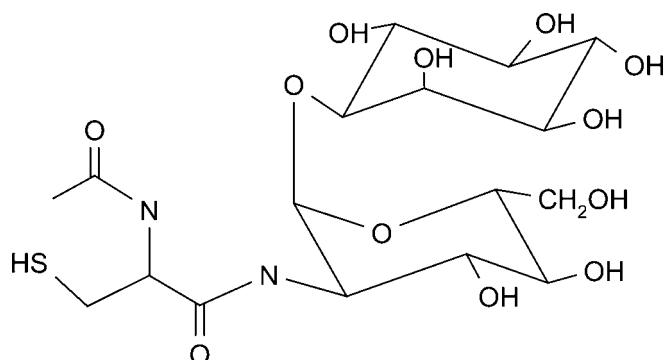


FIG. 1. Structure of mycothiol (1-D-myo-inosityl-2-(L-cystinyl)amido-2-deoxy- $\alpha$ -D-glucopyranoside, AcCys-GlcN-Ins, MSH).

TABLE I  
Crystallographic statistics for structure determination

Crystal	Native	UNO3
Space group	P <sub>1</sub>	P <sub>1</sub>
Cell dimensions		
$a, b, c$ (Å)	56.8, 74.0, 85.6	57.2, 73.8, 85.6
$\alpha, \beta, \gamma$ (Å)	102.1, 108.2, 97.2	101.6, 108.1, 97.4
Wavelength (Å)	1.0000	1.5418
Resolution (Å)	40–1.7 (1.79–1.70) <sup>a</sup>	40–2.5 (2.59–2.50)
Completeness (%)	96.3 (94.7)	94.3 (91.5)
$R_{\text{sym}}$ (%) <sup>b</sup>	5.0 (29.6)	7.6 (23.1)
$(I/\sigma(I))$	5.3 (2.2)	9.0 (3.2)
Redundancy	3.9 (3.7)	1.9 (1.8)
Unique reflections	134,270	41,591
Total reflections	1,281,662	470,788
Figure of merit <sup>c</sup>		0.37–0.60
Number of protein atoms	8364	
Number of solvent atoms	760	
Average B factors (protein/solvent) (Å <sup>2</sup> )	22.2/31.5	
$R_{\text{cryst}}$ <sup>d</sup>	0.194	
$R_{\text{free}}$ <sup>e</sup>	0.228	

<sup>a</sup> All values in parentheses are for highest resolution shell.

<sup>b</sup>  $R_{\text{sym}} = \sum I - \langle I \rangle / \sum I$ , where  $I$  is the observed intensity and  $\langle I \rangle$  is the average intensity obtained from multiple observations of symmetry related reflections.

<sup>c</sup> Two values are given, the first after substructure solution, the second after solvent flattening.

<sup>d</sup>  $R_{\text{cryst}} = \sum |F_o - F_c| / \sum F_o$ , where  $F_o$  and  $F_c$  are the observed and calculated structure factor amplitudes, respectively.

<sup>e</sup>  $R_{\text{free}}$  was calculated as for  $R_{\text{cryst}}$  with 5% of the data omitted from structural refinement.

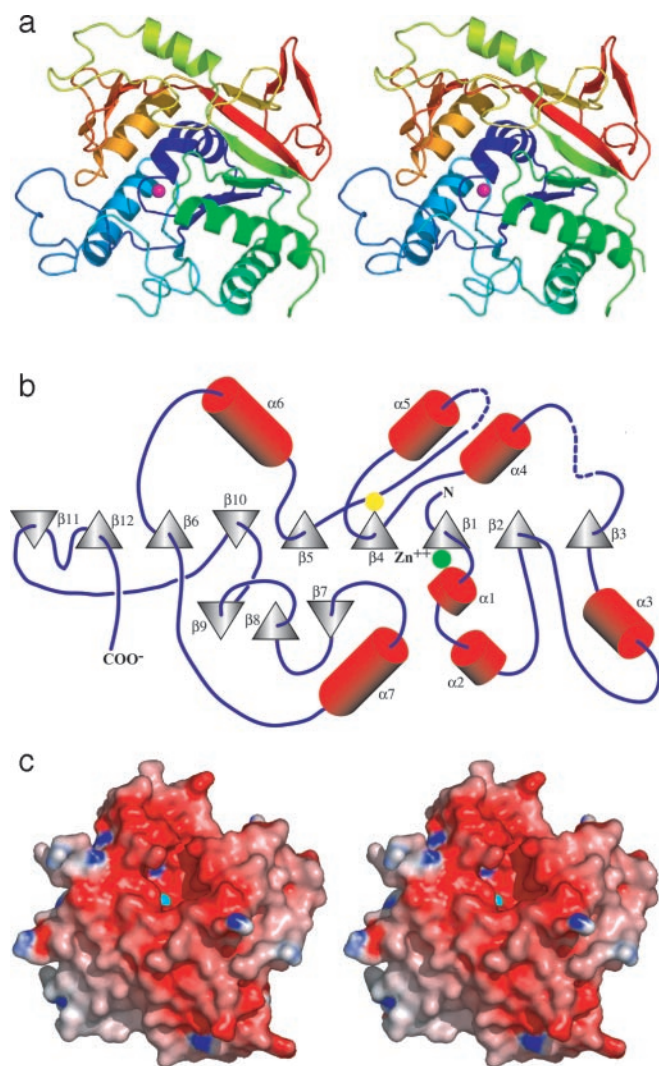


**FIG. 2. Overall structure of MshB.** *a*, stereo representation of one of four MshB molecules present in the crystallographic asymmetric unit. The coloring is blue at the N terminus to red at the C terminus. The catalytic zinc is shown as a magenta sphere. *b*, secondary structure present in the structure of MshB, showing the large central mixed  $\beta$ -sheet and lactate dehydrogenase (Rossmann) fold. The green circle denotes the location of two of the zinc binding ligands (His-13 and Asp-16) and of the general base for the proposed catalytic mechanism (Asp-15) (Fig. 4). The yellow circle represents the location of the third zinc binding ligand (His-147) and the electrophile for the catalytic mechanism (His-144). Broken lines in the chain are used to show areas of untraceable protein chain. *c*, electrostatic surface of MshB. Blue shows areas of positive electronegativity, and red shows areas of negative electronegativity. The catalytic zinc is shown as a cyan sphere deep in the hole surrounding the very electronegative active site.

one of which is also within hydrogen-bonding distance to the carboxylate of Asp-15, a proposed catalytic residue (see Fig. 3).

**Electrostatic Surface Potential of the Enzyme**—The substrate for MshB is 1-*D*-myo-inositol 2-acetamido-2-deoxy- $\alpha$ -*D*-glucopyranoside, a molecule that is highly hydrophilic (see Fig. 4). Not surprisingly, the active site and substrate binding pocket of MshB is also hydrophilic and electronegative, having three carboxylate groups (Asp-15, Asp-95, and Asp-146), three hydroxyl groups (Ser-20, Tyr-142, and Ser-260), one amide from the side chain of Gln-247, four main chain carbonyls (Gly-140, Tyr-142, Glu-213, and Ile-214), and two positively charged residues (Arg-68 and His-144) (Figs. 2c and 3a). Many carbohydrate-binding molecules have similar constellations of hydrophilic residues that form hydrogen-bonding interactions to the sugar hydroxyl groups (27).

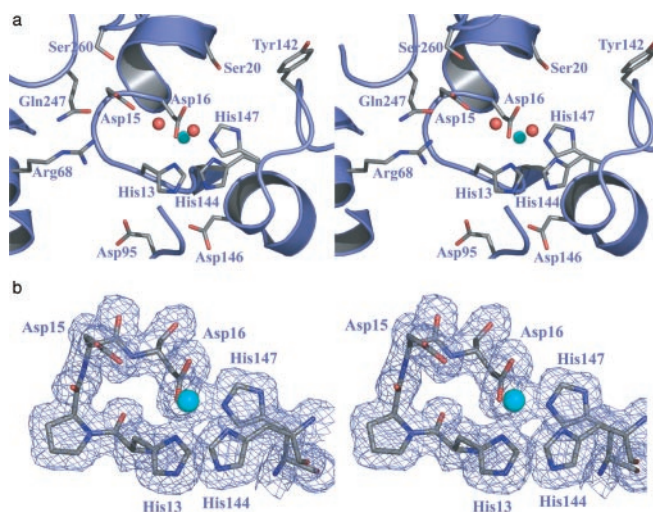


**FIG. 3. The active site of MshB.** *a*, active site representation of one of the MshB molecules in the asymmetric unit. The catalytic zinc is shown as a cyan sphere, and two zinc-bound water molecules are shown as red spheres. The leftmost water molecule is within 2.83 Å of the catalytic Asp-15, and both water molecules are within 3 Å of the metal ion. The other metal ligands are 2.10 (His-13), 2.07 (Asp-16), and 2.13 Å (His-147) from the metal. Orientation of the molecule is the same as in Fig. 2. *b*, representative electron density from the active site region of MshB. The map shown is a  $\sigma_A$ -weighted  $2F_o - F_c$  ( $\alpha_{\text{calc}}$ ) map, contoured at  $1\sigma$ .

## DISCUSSION

**The Active Site of MshB Is Similar to That of a Metalloprotease**—The deacetylation reaction catalyzed by MshB is very similar to that catalyzed by a protease cleaving a peptide bond. It was therefore not completely surprising that the arrangement of residues in the active site of MshB was very similar to that of a metalloprotease. The crystal structures of several metalloproteases, including thermolysin and carboxypeptidase A, have been known for a long time (Protein Data Bank accession codes 4TLN and 5CPA). These enzymes generally employ a metal chelated by three protein ligands (usually two histidines and a glutamate) and a general base carboxylate that activates a water molecule to cleave the peptide bond. A nearly identical constellation of residues in the metalloprotease active site is found in MshB deacetylase (Fig. 3). The ligands on the zinc are two histidines (His-13 and -147) and an aspartate (Asp-16), which differs from the usual glutamate in the metalloproteases. The activating general base is Asp-15, a feature that is unique among  $\text{Zn}^{2+}$  hydrolases.<sup>2</sup> We also see two water molecules in the active site, both in the proximity of the zinc and one near Asp-15, which presumably is the nucleophilic water molecule. The other water molecule is most likely displaced by an incoming substrate. Unlike the water molecule arrangement viewed in carboxypeptidase A, the two water molecules here appear to be uniquely bound and are not two positions with partial occupancy (28). The fact that both water molecules are present can be further verified by a calculation of the valence bond summation in which both water molecules are required to approximate the expected +2 oxidation state of zinc (29). Zinc was chosen as the active site metal for three reasons: 1) metal analysis data indicating  $\text{Zn}^{2+}$ ,<sup>3</sup> 2) a positive  $\text{Zn}^{2+}$  x-ray fluorescence scan, and 3) because zinc commonly adopts a coordination geometry identical to that seen here (30).

The active site region of the enzyme is extremely electronegative (Fig. 2c). A lone exception to this is Arg-68, which flanks one side of the active site (Fig. 3a). This residue is conserved

<sup>2</sup> D. S. Auld, personal communication.

<sup>3</sup> G. Newton and R. C. Fahey, unpublished data.

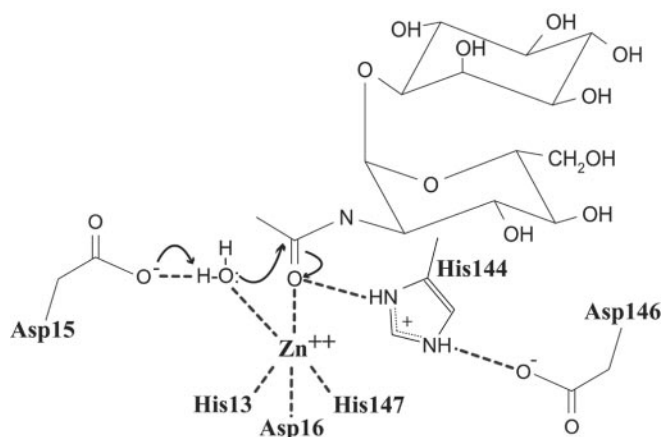


FIG. 4. **Proposed catalytic mechanism for MshB.** The mechanism involves the activation of a water molecule by a general base (Asp-15). Zinc and an electrophile (His-144) are used to stabilize the tetrahedral intermediate formed by the addition of the nucleophilic water molecule to the carbonyl group of the substrate.

among related enzymes (phosphatidylinositol glycan, class L (PIG-L), Rv1082) and may be of importance in the binding of sugar substrates since all of these enzymes have this arginine in common with their substrates (see below).

**Proposed Catalytic Mechanism of MshB**—Given the similar disposition of catalytic residues in the active sites of MshB and the zinc metalloproteinases, it is likely that the deacetylase also has a catalytic mechanism similar to that of the proteinases. The metalloproteinase mechanism involves nucleophilic attack of the hydroxyl ion generated with general base assistance of the carboxylate group of the glutamate on the carbonyl carbon of the scissile peptide bond. In all known metalloproteinases, the general base is a glutamate. The glutamate also has the role of general acid in transferring the proton to the nitrogen of the leaving group of the original peptide bond.

In our proposed catalytic mechanism (Fig. 4) of hydrolysis of GlcNAc-Ins, the substrate binds to MshB so that the carbonyl oxygen of the acetyl group replaces the second water molecule on the  $Zn^{2+}$  ion. This leaves the first water molecule in an ideal position for general base-assisted nucleophilic attack of the carbonyl carbon of the acetyl group. The general base is the carboxylate of Asp-15. The tetrahedral transition state would then have a negatively charged oxygen atom that is stabilized by the positively charged  $Zn^{2+}$  and by the imidazolium side chain of His-144. Proton transfer to the nitrogen of the leaving group (GlcN-Ins) would be via the general acid function of the carboxyl group of Asp-15.

This reaction mechanism might be common to other deacetylases as well. In other mycobacteria, there is strong sequence similarity among the MshB homologs, especially in the region of the metal binding ligands and the catalytic residues. Phosphatidylinositol glycan, class L is an enzyme that catalyzes the deacetylation of *N*-acetyl-D-glucosaminylphosphatidylinositol in glycosylphosphatidylinositol anchor biosynthesis. The enzymes from a variety of species have a section of sequence, AHPDDE, that carries the metal binding histidine and aspartate residues, as well as the catalytic general base aspartate (11, 31).

Thus far, it has not been possible to bind substrate analogs or inhibitors to MshB. The product of the deacetylase reaction, GlcN-Ins, does not strongly inhibit the enzyme, nor does it bind with high affinity.<sup>3</sup> Molecular modeling of MSH in the active site of MshB revealed two potential orientations of the GlcNAc-Ins portion of the molecule. Neither was sufficiently compelling for us to be convinced of their validity. However, there were

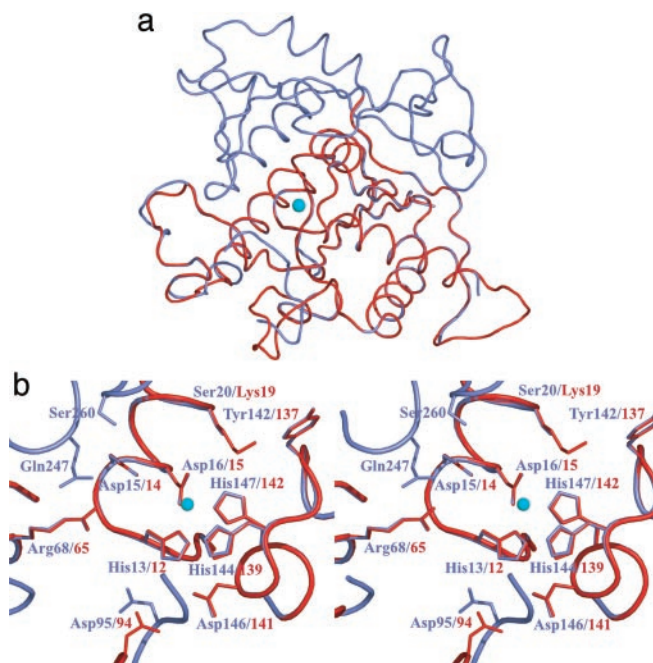


FIG. 5. **Homology model of Mca.** *a*, alignment of the homology model of Mca (red) with MshB (slate). The Mca structure consists of residues 2–180, where significant sequence identity is present and a model could be reliably built. *b*, stereo alignment of the active sites of MshB and Mca. The active site residues including the metal binding ligands and catalytic aspartate are seen to align with the exception of a substitution of Lys-19 (Mca) for Ser-20 (MshB). Coloring is as in A for both the active site structure and labels.

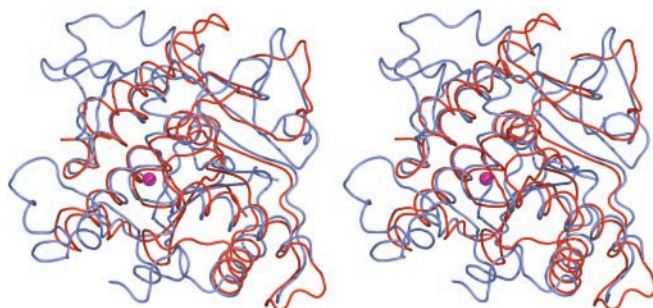


FIG. 6. **Alignment of MshB (slate) with a related protein from *Thermus thermophilus* (TT1542) (red).** Both proteins show similar Rossmann folds with common zinc binding regions. The catalytic zinc is shown as a magenta sphere.

many potential hydrogen-bonding interactions in the vicinity of the two most likely orientations. Removal of the inositol, leaving only GlcNAc as the substrate, reduces the catalytic activity of MshB by 300-fold (11). Clearly, there must be important interactions of the inositol with MshB.

MshB exhibits weak amidase activity toward mycothiol *S*-conjugates, cleaving the bond linking the AcCys residue to GlcN-Ins. The related enzyme, Mca, exhibits high activity with mycothiol *S*-conjugates and very low deacetylase activity with GlcNAc-Ins.<sup>4</sup> Thus, these two enzymes have slightly overlapping functions. Mca plays a key role in the detoxification of electrophiles, which form *S*-conjugates with mycothiol (11), and there is reason to believe that certain antibiotics are detoxified by an MSH-dependent pathway involving Mca (9).<sup>4</sup> Thus, Mca may also be an important target for TB drugs, and its three-dimensional structure is therefore important.

<sup>4</sup> Steffek, M., Newton, G. L., Av-Gay, Y., and Fahey, R. C. (2003) *Biochemistry* **42**, 12067–12076.

*Modeling of Mca Encoded by Open Reading Frame Rv0182*—MshB and Mca share 32% sequence identity overall and 43% over the first 200 residues. Based on this sequence identity, a homology model for the catalytic portion of Mca was constructed (Fig. 5) (33). The model was successfully built up to residue 180, where the sequence identity became too sparse for a successful fit. The homology model showed amazing similarity between the two structures with all pertinent active site residues aligning perfectly, including the metal binding site and the catalytic aspartate. Mca has very low activity toward GlcNAc-Ins; therefore, substrate specificity must be vital. The only major difference in the active sites is the incorporation of Lys-19 in Mca, where Ser-20 was in MshB. This residue may therefore be important in disaccharide binding, in which the serine in MshB interacts with hydroxyls on the sugars, and the lysine in Mca may sterically hinder them. Since the same sugar moiety must bind to Mca, it may bind in a different orientation, or the unfavorable interactions with the sugar alone could be compensated for by additional interactions with the AcCys residue of MSH. These interactions would most likely involve residues that occupy the positions of Gln-247 and Ser-260 in MshB since this is where most of the sequence variation between MshB and Mca occurs, and it was not possible to model this region accurately.

Recently, the structure of a similar protein (TT1542) from *Thermus thermophilus* was determined as part of a structural genomics initiative (34). MshB and TT1542 share 33% identity or strong sequence similarity, although TT1542 is 80 residues shorter in length. The role of TT1542 is unknown, and the assumed active site of the enzyme does not contain a metal atom. The enzymes share a very similar fold and active site residues, and therefore, it is likely that TT1542 has a similar role as a zinc aminohydrolase, although the natural substrate remains unknown (Fig. 6).

The control of reactive oxygen and reactive nitrogen intermediates is extremely important to all organisms. Mycothiol appears to play a major role in protecting mycobacteria against peroxide toxicity (7, 9, 14) and in detoxifying nitric oxide (32). It therefore appeared that drugs directed against MshB might be able to block MSH production, but recent work has shown that in *M. tuberculosis* Erdman (14) and in *Mycobacterium smegmatis* (9), inactivation of the *mshB* gene does not fully block MSH biosynthesis. Another amidase, possibly Mca, apparently has sufficient GlcNAc-Ins deacetylase activity to support a low level of MSH production during exponential growth. If a drug could be found that blocks both deacetylase activities, then MSH production might be effectively eliminated. Alternatively a drug that blocks Mca activity might serve to enhance the toxicity of known antibiotics toward *M. tuberculosis*. The novel fold that MshB (and by homology Mca) contains should prove helpful in the design of such drugs, whereas the similar-

ity of the active sites to known metalloproteinases presents a scaffold from which drug targets can be designed.

*Acknowledgments*—We thank Thomas Earnest and James Holton at Advanced Light Source (ALS) and Mary Ko for technical assistance. J. T. Maynes and M. N. G. James are especially indebted to the Alberta Synchrotron Institute for their support in data collection at the ALS.

#### REFERENCES

- Dye, C., Scheele, S., Dolin, P., Pathania, V., and Raviglione, M. C. (1999) *JAMA (J. Am. Med. Assoc.)* **282**, 677–686
- WHO (1998) *Global Tuberculosis Control*, pp. 1–3, WHO, Geneva, Switzerland
- Amaral, L., Viveiros, M., and Kristiansen, J. E. (2001) *Trop. Med. Int. Health* **6**, 1016–1022
- Newton, G. L., Arnold, K., Price, M. S., Sherrill, C., Delcardayre, S. B., Aharonowitz, Y., Cohen, G., Davies, J., Fahey, R. C., and Davis, C. (1996) *J. Bacteriol.* **178**, 1990–1995
- Misset-Smits, M., van Ophem, P. W., Sakuda, S., and Duine, J. A. (1997) *FEBS Lett.* **409**, 221–222
- Norin, A., Van Ophem, P. W., Piersma, S. R., Persson, B., Duine, J. A., and Jornvall, H. (1997) *Eur. J. Biochem.* **248**, 282–289
- Newton, G. L., Unson, M. D., Anderberg, S. J., Aguilera, J. A., Oh, N. N., delCardayre, S. B., Av-Gay, Y., and Fahey, R. C. (1999) *Biochem. Biophys. Res. Commun.* **255**, 239–244
- Newton, G. L., Av-Gay, Y., and Fahey, R. C. (2000) *Biochemistry* **39**, 10739–10746
- Rawat, M., Newton, G. L., Ko, M., Martinez, G. J., Fahey, R. C., and Av-Gay, Y. (2002) *Antimicrob. Agents Chemother.* **46**, 3348–3355
- Newton, G. L., Koledin, T., Gorovitz, B., Rawat, M., Fahey, R. C., and Av-Gay, Y. (2003) *J. Bacteriol.* **185**, 3476–3479
- Newton, G. L., Av-Gay, Y., and Fahey, R. C. (2000) *J. Bacteriol.* **182**, 6958–6963
- Sareen, D., Steffek, M., Newton, G. L., and Fahey, R. C. (2002) *Biochemistry* **41**, 6885–6890
- Koledin, T., Newton, G. L., and Fahey, R. C. (2002) *Arch. Microbiol.* **178**, 331–337
- Buchmeier, N. A., Newton, G. L., Koledin, T., and Fahey, R. C. (2003) *Mol. Microbiol.* **47**, 1723–1732
- Newton, G. L., and Fahey, R. C. (2002) *Arch. Microbiol.* **178**, 388–394
- Leslie, A. G. W. (1992) *Joint CCP4 + ESF-EAMCB Newsletter on Protein Crystallography*, No. 26, CCP4, York, UK
- Evans, P. R. (1993) *Proceedings of the CCP4 Study Weekend on Data Collection and Processing*, pp. 114–122, CCP4, York, UK
- Bailey, S. (1994) *Acta Crystallogr. Sect. D Biol. Crystallogr.* **50**, 760–763
- Terwilliger, T. C. (2001) *Acta Crystallogr. Sect. D Biol. Crystallogr.* **57**, 1763–1775
- Terwilliger, T. C. (2002) *Acta Crystallogr. Sect. D Biol. Crystallogr.* **58**, 1937–1940
- Perrakis, A., Morris, R., and Lamzin, V. S. (1999) *Nat. Struct. Biol.* **6**, 458–463
- Murshudov, G. N., Vagin, A. A., and Dodson, E. J. (1997) *Acta Crystallogr. Sect. D Biol. Crystallogr.* **53**, 240–255
- McRee, D. E. (1999) *J. Struct. Biol.* **125**, 156–165
- Delano, W. L. (2002) *The PyMol Molecular Graphics System*, Delano Scientific, San Carlos, CA
- White, J. L., Hackert, M. L., Buehner, M., Adams, M. J., Ford, G. C., Lentz, P. J., Smiley, I. E., Steindel, S. J., and Rossmann, M. G. (1976) *J. Mol. Biol.* **102**, 759–779
- Holm, L., and Sander, C. (1993) *J. Mol. Biol.* **233**, 123–138
- Quioco, F. A. (1993) *Biochem. Soc. Trans.* **21**, 442–448
- Rees, D. C., Lewis, M., and Lipscomb, W. N. (1983) *J. Mol. Biol.* **168**, 367–387
- Brown, I. D. (1996) *J. Appl. Crystallogr.* **29**, 479–480
- Roe, R. R., and Pang, Y. P. (1999) *J. Mol. Model.* **5**, 134–140
- Chang, T., Milne, K. G., Guther, M. L., Smith, T. K., and Ferguson, M. A. (2002) *J. Biol. Chem.* **277**, 50176–50182
- Vogt, R. N., Steenkamp, D. J., Zheng, R., and Blanchard, J. S. (2003) *Biochem. J.* **374**, 657–666
- Schwede, T., Kopp, J., Guex, N., and Peitsch, M. C. (2003) *Nucleic Acids Res.* **31**, 3381–3385
- Handa, N., Terada, T., Kamewari, Y., Hamana, H., Tame, J. R., Park, S. Y., Kinoshita, K., Ota, M., Nakamura, H., Kuramitsu, S., Shirouzu, M., and Yokoyama, S. (2003) *Protein Sci.* **12**, 1621–1632